Regular Article

$LaFe_{11.6}Si_{1.4}H_y$/Sn magnetocaloric composites by hot pressing

Heng Zhang [a,b,c], Jian Liu [a,b,*], Mingxiao Zhang [a,b,*], Yanyan Shao [a,b], Yang Li [a,b,c], Aru Yan [a,b]

[a] Key Laboratory of Magnetic Materials and Devices, Ningbo Institute of Material Technology and Engineering, CAS, Ningbo 315201, China
[b] Zhejiang Province Key Laboratory of Magnetic Materials and Application Technology, Ningbo Institute of Material Technology and Engineering, CAS, Ningbo 315201, China
[c] School of Materials Science and Engineering, Shanghai University, Shanghai 200072, China

A B S T R A C T

We report on the microstructure, mechanical properties, magnetocaloric effect and thermal transfer performance of $LaFe_{11.6}Si_{1.4}H_y$/Sn composites prepared by hot pressing. The liquid Sn forms a homogenous continuous matrix but does not react with $LaFe_{11.6}Si_{1.4}H_y$ grains during compacting. By controlling pressing temperature, a set of composites combined high entropy change values of 10–13 J/kg K at 2 T with high thermal conductivity of about 7 W/mK has been obtained in a magnetostructural transition range of 1–17 °C.

As an emerging type of environment friendly and energy efficient refrigeration technology, magnetic refrigeration based on the magnetocaloric effect (MCE) has been considered as an alternative technology to the existing vapor compression refrigeration [1]. The cubic $NaZn_{13}$-type (i.e. 1:13 phase) La(Fe, Si)$_{13}$-based compounds are regarded as one of the most promising magnetic refrigeration materials around room temperature due to its low cost, non-toxicity, continuously adjustable Curie temperature (T_c) and large entropy change (ΔS) [2]. By hydrogen absorption, T_c is increased up to room temperature; meanwhile the first-order magneto-volume transition and associated large MCE can be maintained in the hydrides [3]. However, hydrogen decrepitation and powderization inevitably occur in La-Fe-Si compounds during hydrogenation. In order to enhance heat transfer capability, an appropriate method should be considered to assemble hydride powders into a bulk material [4]. Several technologies have been adopted to prepare bulk La(Fe, Si)$_{13}$-based composites by powder metallurgical process, such as epoxy bonding [5], electroless copper plating [6] and hot pressing (HP) with amorphous particles [7]. Epoxy-bonded La-Fe-Si composites exhibit a higher compressive strength than that of cast bulk, which makes the composites possible to be machined into thin plates more feasibly. But epoxy with a rather low thermal conductivity brings about a negative influence on the composite applications [5]. Metal-based La(Fe, Si)$_{13}H_y$/Cu composites by HP have shown a balance between the good mechanical properties and high thermal conductivity [6]. Unfortunately, both the formation of extra phase by significant high-temperature inter-diffusion, and the press-induced particle cracking lead to the decreased ΔS [8]. Although Pd-based amorphous matrix becomes softer at its glass transition temperature (T_g) and thus leads to less fractured La(Fe, Si)$_{13}$-based particles by compaction, the constitutive element of Pd is costly for mass production and the T_g about 300 °C is too high to store hydrogen [7]. The search for materials with high thermal conductivity and low softening/melting point is very desirable for the compaction with La(Fe, Si)$_{13}H_y$ powders. In this work, the pure metal Sn with low melting point (T_m = 232 °C) and high thermal conductivity (λ = 66.6 W/mK) is used to prepare $LaFe_{11.6}Si_{1.4}H_y$/Sn composites by HP process.

$LaFe_{11.6}Si_{1.4}$ flakes were prepared by strip casting technique as described earlier [9]. The as-cast flakes were annealed at 1050 °C for 24 h, and then crushed to coarse particles for hydrogenation. The hydrogen absorption experiment was carried out in a furnace filled with 2 bar H_2 atmosphere at 300 °C for 5 h, to saturate the H concentration. Afterwards, the hydrogenated $LaFe_{11.6}Si_{1.4}H_y$ coarse particles were further ground into finer powders in a size range of 50 – 75 μm. The commercial Sn powders in size smaller than 43 μm was selected. The weight ratio of $LaFe_{11.6}Si_{1.4}H_y$ to Sn powders is kept as 4:1. The mixed powders were hot pressed at 200–250 °C under an applied pressure of 200 MP in vacuum for 2 min. The resulting hot-pressed samples have a cylinder shape with 13 mm in diameter and 5 mm in height. By weighting the sample mass before and after hot pressing, it is estimated that a small amount of Sn was exuded out of the sample under pressure, and the finally maintained Sn accounts for about 15% in mass fraction. The microstructure was observed by scanning electron microscope (SEM). The elemental mapping images were observed by energy-dispersive spectroscopy (EDS) in SEM. Compressive strength was tested in a universal testing machine. Magnetic properties were measured by a superconducting quantum interference device (SQUID) vibrating sample magnetometer.

* Corresponding authors at: Key Laboratory of Magnetic Materials and Devices, Ningbo Institute of Material Technology and Engineering, CAS, Ningbo 315201, China.
E-mail addresses: liujian@nimte.ac.cn (J. Liu), mxzhang@nimte.ac.cn (M. Zhang).

Thermal conductivity was measured at room temperature using a laser-flash thermal conductivity apparatus (LFA). The density of samples was examined by the Archimedes method.

Fig. 1 shows the microstructure of $LaFe_{11.6}Si_{1.4}H_y$/Sn composite hot-pressed at 225 °C. It can be seen that $LaFe_{11.6}Si_{1.4}H_y$ particles (grey area) are well coated by Sn surroundings (white area), while the pores architecture (black area) still exists (Fig. 1a). The composite density calculated by the Archimedes method is 6.40 g/cm^3 (listed in Table 1), while the theoretical full density of composites is 7.05 g/cm^3. The porosity of the sample of about 9.2% is consistent with the microstructural observation. Upon hot pressing, large size particles are prone to be crushed into smaller pieces. Interestingly, the molten Sn enables to repair fragments through flowing into the fracture gap within each particle under the applied pressure (Fig. 1b). This indicates a good wettability between liquid Sn and solid $LaFe_{11.6}Si_{1.4}H_y$. Furthermore, we found the absence of newly formed phase detected in the interface of $LaFe_{11.6}Si_{1.4}H_y$/Sn. From EDS elemental mapping (Fig. 1c), there is no notable atomic inter-diffusion between Fe and Sn. This is in contrast with the case of hot-pressed $La(FeSi)_{13}$/Cu composites, where a new intermetallic Fe_4Cu_3 phase was formed above 600 °C [8]. Since there is no data available on the diffusion coefficient between Cu and 1:13 phase, we assess the diffusion velocity by taking the chemical diffusion coefficient of Cu atoms in the α-Fe phase, which was determined to be $D_{Cu/Fe} = 0.71 \times 10^{-14}$ cm^2/s at 650 °C [10]. It should be noted that even a small amount of Cu solidly dissolves in a single 1:13 phase, a drastic decrement of ΔS can take place [11,12]. In comparison, a much lower diffusivity for Sn in α-Fe of $D_{Sn/Fe} = 2.0 \times 10^{-19}$ cm^2/s at 400 °C was measured [13]. Below 300 °C, there is almost no diffusion and very limited solubility between Fe and Sn, as proposed by Rusakov et al. [14]. Therefore, the low degree of diffusion in Fe/Sn at low temperatures, as well as the difficulty to form new phase in a short time imply that the present $LaFe_{11.6}Si_{1.4}H_y$/Sn has the potential to keep good MCE. In this case, Sn flows through 1:13 grains without reactive sintering effect.

Fig. 2 shows the macrophotograph in the vertical section of the sample hot pressed at 250 °C (a) and elemental maps in selective areas of the sample (b–d). A homogeneous distribution of composite architecture can be observed in various parts, which implies the consistency of the MCE and mechanical properties in the whole sample. For the hot-pressed Nd-Fe-B magnets, the high densification and good homogeneity are realized by Nd-rich liquid phase along the grain boundaries [15,16], while the microstructural segregation from end surfaces to inner part is generally caused by uneven hot plastic deformation in texturing process [17]. As for our $LaFe_{11.6}Si_{1.4}H_y$/Sn composites, Sn acts as a ductile binder to reduce the amount of pores during compacting. On the other hand, since the hot deformation is not necessary for $LaFe_{11.6}Si_{1.4}H_y$/Sn composites, the HP samples demonstrate the homogenous microstructure, as well as their associated mechanical and MCE properties as described in follows.

Compressive stress-strain curves for samples compacted at 200 and 250 °C are shown in Fig. 3. It is found that $LaFe_{11.6}Si_{1.4}H_y$/Sn composites pressed at 250 °C exhibits the compressive strength of 170 MPa, which has the similar level to that in polymer-bonded $LaFe_{11.7}Si_{1.3}C_{0.2}H_{1.8}$ (~160 MPa) [18]. The sample compacted at 200 °C (far below the melting temperature of Sn) has a lower ultimate stress of about 90 MPa and lower modulus due to its poorer densification. The smooth surface in the sample compacted at 250 °C is quite different from the matte surface observed in the 200 °C HP sample, as clearly seen in the inset of Fig. 3. The enhanced mechanical properties evidence that with the increased compacting temperature, more porous spaces can be filled by Sn liquid similar to liquid-phase sintering. Also, we found a good repeatability in compressive test data for different sample parts (not shown here), which further reflects the homogenous microstructure in our HP samples.

Table 1
Magnetic entropy change (ΔS), Curie temperature (T_c), thermal conductivity (λ) and density (ρ) of $LaFe_{11.6}Si_{1.4}H_y$/Sn samples hot pressed at different temperatures.

HP temperature (°C)	225	233	242	250
ΔS (J/kg K), 2 T	11.8	10.2	12.6	12.5
T_c (°C)	17	8	5	1
λ (W/mK)	7.9	6.6	7.1	6.8
ρ (g/cm^3)[a]	6.40	6.35	6.36	6.42

[a] Full density of $LaFe_{11.6}Si_{1.4}H_y$/Sn composites is 7.05 g/cm^3.

Fig. 4 exhibits magnetization vs. field and entropy change vs. temperature curves for HP composites (c). For comparison, the magnetostructural transition and MCE characters of starting $LaFe_{11.6}Si_{1.4}H_y$ loose powders (a) and mixed powders of $LaFe_{11.6}Si_{1.4}H_y$ with Sn simply hold at 250 °C for 2 min without press (b) are investigated. The pure $LaFe_{11.6}Si_{1.4}H_y$ powder sample that transforms sharply with a first-order manner accompanying by a small hysteresis (2.4 J/kg) shows the maximum value of ΔS (15.3 J/kg K in 2 T). Upon heating with Sn up to 250 °C, the first order transition feature becomes smeared, which results in a less magnetic hysteresis (2.2 J/kg) and apparently dropped ΔS (10.1 J/kg K in 2 T). When considering the mass fraction of Sn unparticipating transformation as 15%, the net value of ΔS would have to be as high as 13 J/kg K for the composite sample. The reason for the greatly decreased MCE could be the inhomogeneous dehydrogenation process. The partial dehydrogenation by heat treatment leads to the T_c value decreased from 60 to 30 °C. Not only temperature, but pressing also plays a role to the dehydrogenation. This can be evidenced by the further decreased T_c (1 °C) in HP sample (Fig. 4c). However, the nature of first order magnetostructural transition and large MCE are somehow recovered by hot pressing. The magnetic hysteresis is 5.2 J/kg and maximum value of ΔS in 2 T is 12.5 J/kg K for the sample hot-pressed at 250 °C. The ΔS for the composite sample is very close to the effective value, which implies almost no MCE degradation occurring in such a homogenous dehydrogenation processing. As pressing reduces the particle size approximately from 50 to 10 μm, the smaller particles favors a fast desorption rate and homogenous hydrogen distribution [19]. It has been extensively reported that in La-Fe-Si-based compounds, the finer 1:13 particle size, the less MCE due to the diminishing of grain boundaries constraint and removal of extrinsic hysteresis [2,

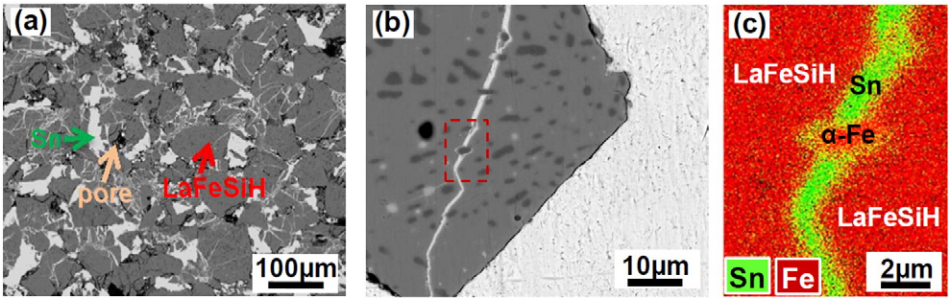

Fig. 1. SEM backscattered electron image for $LaFe_{11.6}Si_{1.4}H_y$/Sn hot-pressed at 225 °C (a). Enlarged micrograph of a single $LaFe_{11.6}Si_{1.4}H_y$ particle surrounded by Sn matrix shows a compacting-caused crack filled by Sn (b). The area of dashed box in (b) is elementally mapped by EDS shown in (c).

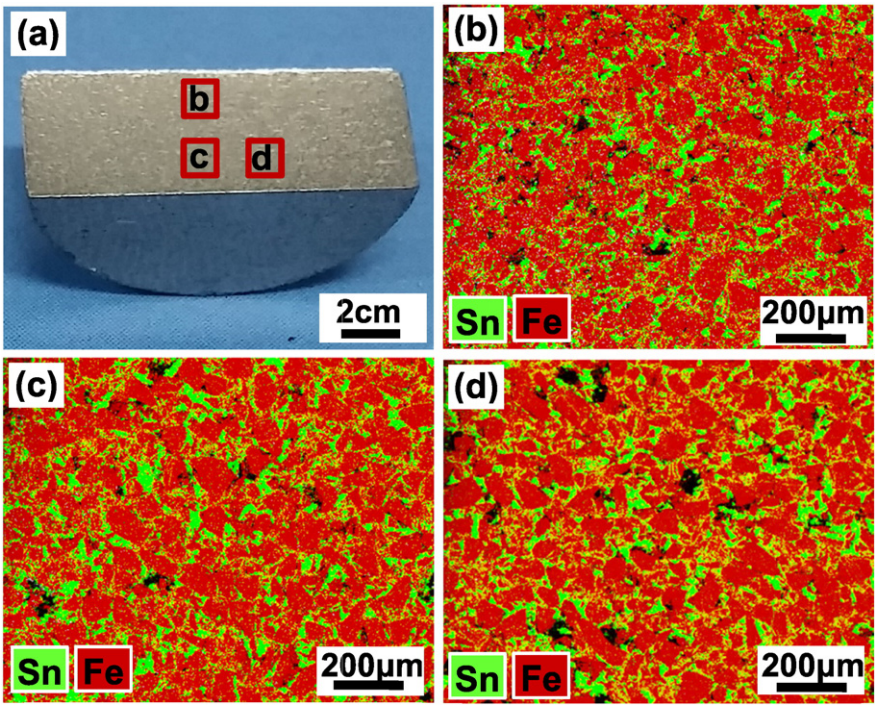

Fig. 2. Vertical section of the 250 °C HP sample (a) and SEM-EDS elemental mapping images for different parts of the sample (b, c, d).

20]. Interestingly, an abnormality that smaller particles size nearly does not impair the high MCE, happens in the present $LaFe_{11.6}Si_{1.4}H_y$/Sn composites. It can be ascribed this phenomenon as the constraint effect from Sn surroundings. On the other hand, as the bulk modulus of La-Fe-Si compound (~125 GPa) [21] is much higher than that of Sn (~57 GPa) [22], the existance of Sn should not block the magnetovolum transition and thus the magneto-elastic dominately contribution contributes to the large MCE.

Comparing the ambient MCE with previously reported La(Fe, Si)$_{13}$-based *bulks*, the ΔS value of the HP sample (12.5 J/kg K in 2 T at 1 °C) is higher than that measured in the similar T_c range, such as sintered $LaFe_{11.05}Co_{0.84}Si_{1.1}$ alloy (9 J/kg K in 2 T at 1.2 °C) [23], polymer-bonded $La_{0.9}Ce_{0.1}Fe_{11.41}Mn_{0.29}Si_{1.3}H_{1.8}$ composite (7.9 J/kg K in 2 T at 8 °C) [24] and Fe-rich $LaFe_{12.1}Co_{0.8}Si_{1.2}$ dual-phase alloy (7.9 J/kg K in 2 T at 6 °C) [25]. Considering the practical application, it is more meaningful to know the volumetric entropy change of magnetocaloric materials.

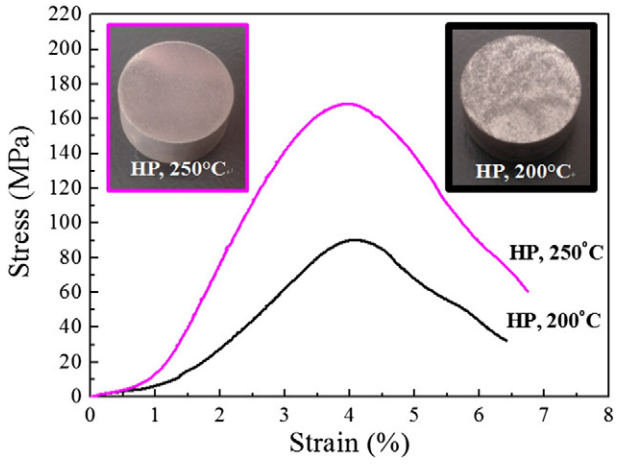

Fig. 3. Compressive stress–strain curves for $LaFe_{11.6}Si_{1.4}H_y$/Sn composites hot pressed at 200 and 250 °C. Insets are the sample photographs.

According to the density listed in Table I, the volumetric ΔS_v of our HP composites is calculated to be 80.3 kJ/m^3 K. It still keeps a higher value than that observed in polymer-bonded La(Fe, Mn, Si)$_{13}H_y$ (55–65 kJ/m^3 K) [26] and $LaFe_{11.7}Si_{1.3}C_{0.2}H_{1.8}$ (55 kJ/m^3 K) composites [18], and metal-matrixed $LaFe_{11.6}Si_{1.4}H_y$/Cu composites (70 kJ/m^3 K) [6].

Table 1 gives the magnetic entropy change, Curie temperature, thermal conductivity and density of composites HP at different temperatures. As hydrogen content lowers with the increase of pressing temperature, T_c can be adjusted by means of controlling HP temperature, thus leading to cascade magnetic refrigerants with tunable magnetostructural transitions. Meaning while, the level of ΔS keeps in the range of 10–13 J/kg K. The most significance of metal-based magnetocaloric composites is the high thermal transport properties superior to polymer-bonded composites. For example, the λ value of for the epoxy-bonded La-Fe-Co-Si composites is about 2.7 W/mK at 300 K [27]. Even using thermal conductive silver-based epoxy, the λ value is only up to 5 W/mK for La(Fe, Mn, Si)$_{13}H_y$ polymer composites [26]. Due to the introduction of continuous Sn matrix, the current composites display a high room-temperature thermal conductivity of 7.9, 6.6, 7.1 and 6.8 W/mK for different temperature hot-pressed at 225, 233, 242 and 250 °C, respectively. One notices that a peculiarly higher thermal conductivity of 7.9 W/mK was observed in the sample HP at 225 °C. This might be related to its T_c (17 °C) near room temperature, where the large magneto-volume effect is more pronounced [28]. However, as known from the fully condensed $LaFe_{11.6}Si_{1.4}$ cast sample with an even higher λ value of 9.7 W/mK at 300 K [6], it is assumed that the thermal resistance caused by the appearance of porosity in the composite sample has an unbeneficial effect on further enhancing heat transfer ability.

In summary, $LaFe_{11.6}Si_{1.4}H_y$/Sn hot-pressed composites show the homogenous microstructure, good performance in magnetocaloric and mechanical properties, as well as thermal conductivity. A feasible route to fabricate magnetocaloric materials with different Curie temperatures by changing pressing temperature is proposed.

This work is supported by the National Natural Science Foundation of China (Grant Nos. 51371184 and 51531008) and Zhejiang Provincial Natural Science Foundation of China (Grant No. LR14E010001 and LY16E010002).

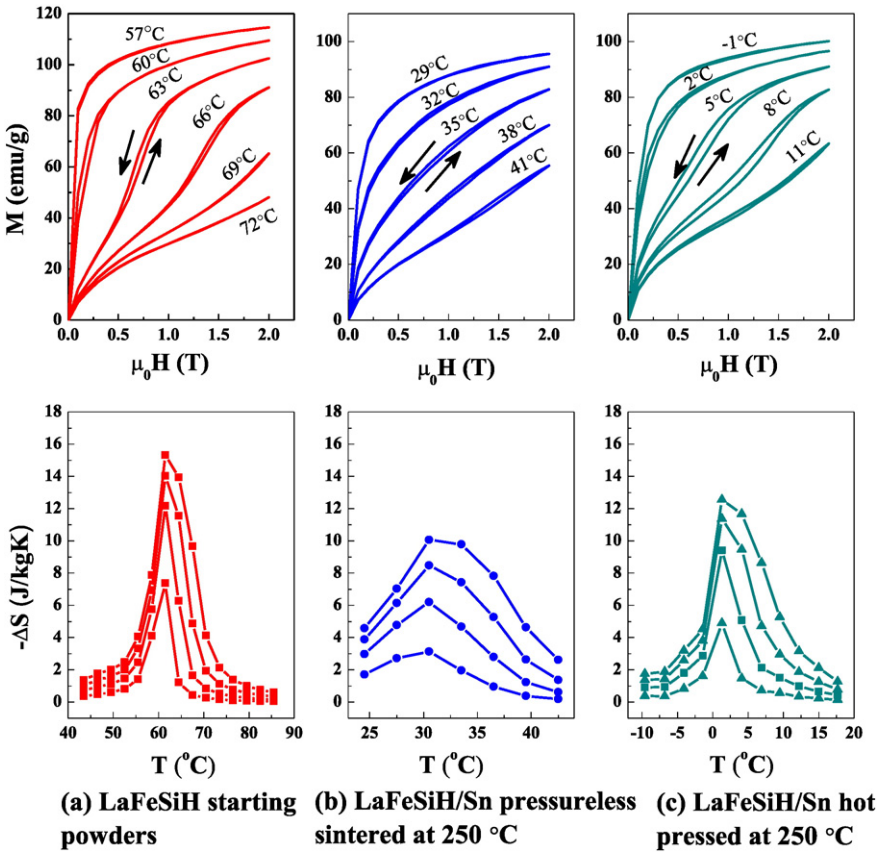

Fig. 4. Selective isothermal magnetization curves (up row) and magnetic entropy changes as a function of temperature (bottom row) for $LaFe_{11.6}Si_{1.4}H_y$ starting powders (a), $LaFe_{11.6}Si_{1.4}H_y$/Sn composites prepared by pressureless sintering at 250 °C for 2 min (b) and by hot pressed at 250 °C for 2 min (c). Entropy change vs. temperature plots under a magnetic field of 0.5, 1.0, 1.5 and 2 T are shown from the bottom up.

References

[1] O. Gutfleisch, M.A. Willard, E. Bruck, C.H. Chen, S.G. Sankar, J.P. Liu, Adv. Mater. 23 (2011) 821–842.
[2] J. Liu, J. Moore, K. Skokov, M. Krautz, K. Löwe, A. Barcza, M. Katter, O. Gutfleisch, Scr. Mater. 67 (2012) 584–589.
[3] A. Fujita, S. Fujieda, Y. Hasegawa, K. Fukamichi, Phys. Rev. B 67 (2003) 104416.
[4] M. Kuz'min, Appl. Phys. Lett. 90 (2007) 251916.
[5] K.P. Skokov, D.Y. Karpenkov, M.D. Kuz'min, I.A. Radulov, T. Gottschall, B. Kaeswurm, M. Fries, O. Gutfleisch, J. Appl, Phys. 115 (2014) 17A941.
[6] J. Lyubina, U. Hannemann, L.F. Cohen, M.P. Ryan, Adv. Energy Mater. 2 (2012) 1323–1327.
[7] M. Krautz, A. Funk, K.P. Skokov, T. Gottschall, J. Eckert, O. Gutfleisch, A. Waske, Scr. Mater. 95 (2015) 50–53.
[8] J. Liu, M.X. Zhang, Y.Y. Shao, A. Yan, IEEE Trans. Magn. 51 (2015) 2501502.
[9] M.X. Zhang, J. Liu, Y. Zhang, J.D. Dong, A. Yan, K.P. Skokov, O. Gutfleisch, J. Magn. Magn. Mater. 377 (2015) 90–94.
[10] M.S. An, R.P. Agarwala, J. Appl. Phys. 37 (1966) 4248.
[11] M.F. Md Din, J.L. Wang, R. Zeng, P. Shamba, J.C. Debnath, S.X. Dou, Intermetallics 36 (2013) 1–7.
[12] B. Gao, F.X. Hu, J. Wang, J. Shen, J.R. Sun, B.G. Shen, J. Appl, Phys. 105 (2009) 07A916.
[13] D.N. Torres, R.A. Perez, F. Dyment, Acta Mater. 48 (2000) 2925–2931.
[14] V.S. Rusakov, I.A. Sukhorukov, A.M. Zhankadamova, K.K. Kadyrzhanov, J. Surf, Invest. X-ray, Synchrotron Neutron Tech. 5 (2011) 601–609.
[15] W. Lipiec, H.A. Davies, J. Alloys, Compd. 491 (2010) 694–697.
[16] R.K. Mishra, J. Appl. Phys. 62 (1987) 967–971.
[17] W.Z. Yin, R.J. Chen, X. Tang, X. Tang, D. Lee, A. Yan, IEEE Trans. Magn. 50 (2014) 2100704.
[18] H. Zhang, Y.J. Sun, E. Niu, F.X. Hu, J.R. Sun, B.G. Shen, Appl. Phys. Lett. 104 (2014) 062407.
[19] G.F. Wang, L.J. Mu, X.F. Zhang, Z.R. Zhao, J.H. Huang, J. Appl. Phys. 115 (2014) 143903.
[20] F.X. Hu, L. Chen, J. Wang, L.F. Bao, J.R. Sun, B.G. Shen, Appl. Phys. Lett. 100 (2012) 072403.
[21] E. Valiev, I. Berger, V. Voronin, V. Glazkov, A. Kaloyan, K. Podurets, Phys. Solid State 56 (2014) 14–16.
[22] W. Martienssen, in: W. Martienssen, H. Warlimont (Eds.), Springer Handbook of Condensed Matter and Materials Data, Springer, Berlin Heidelberg, New York 2005, pp. 45–158.
[23] M. Katter, Zellmann, G.W. Reppel, K. Uestuener, in: P.W. Egolf, E. Bruck, K.G. Sandenman, et al., (Eds.), Proceedings of the Third IIF-IIR International Conference on Magnetic Refrigeration at Room Temperature, Institut International du Froid Publishing, Des Moines, IA 2009, pp. 83–88.
[24] W. Xia, J.H. Huang, N.K. Sun, C.L. Lui, Z.Q. Ou, L. Song, J. Alloys Compd. 635 (2015) 124–128.
[25] Y.Y. Shao, M.X. Zhang, H.B. Luo, A. Yan, J. Liu, Appl. Phys. Lett. 107 (2015) 152403.
[26] I.A. Radulov, K.P. Skokov, D.Y. Karpenkov, T. Gottschall, O. Gutfleisch, J. Magn. Magn. Mater. 396 (2015) 228–236.
[27] B. Pulko, J. Tušek, J.D. Moore, B. Weise, K. Skokov, O. Mityashkin, A. Kitanovski, C. Favero, P. Fajfar, O. Gutfleisch, J. Magn. Magn. Mater. 375 (2015) 65–73.
[28] I.A. Radulov, K.P. Skokov, D.Y. Karpenkov, T. Braun, O. Gutfleisch, IEEE Trans. Magn. 51 (2015) 2501204.